He *et al. Soft Sci.* **2025**, *5*, 5
DOI: 10.20517/ss.2024.50

Soft Science

Review Article

Open Access

Check for updates

A review: exploring the designs of bio-bots

Shuchang He[1,#], Songyuan Liu[1,#], Xuegang Li[2], Maosheng Ye[1], Huaping Wu[2], Jizhou Song[1,3,*]

[1]Key Laboratory of Soft Machines and Smart Devices of Zhejiang Province, State Key Laboratory of Brain-Machine Intelligence, Department of Engineering Mechanics, Zhejiang University, Hangzhou 310027, Zhejiang, China.
[2]Institute of Advanced Manufacturing Technology and Modern Design, College of Mechanical Engineering, Zhejiang University of Technology, Hangzhou 310023, Zhejiang, China.
[3]Department of Rehabilitation Medicine, The First Affiliated Hospital School of Medicine, Zhejiang University, Hangzhou 310003, Zhejiang, China.
[#]Authors contributed equally.

[*]**Correspondence to:** Prof. Jizhou Song, Key Laboratory of Soft Machines and Smart Devices of Zhejiang Province, State Key Laboratory of Brain-Machine Intelligence, Department of Engineering Mechanics, Zhejiang University, 38 Zheda Road, Xihu District, Hangzhou 310027, Zhejiang, China. E-mail: jzsong@zju.edu.cn

How to cite this article: He, S.; Liu, S.; Li, X.; Ye, M.; Wu, H.; Song, J. A review: exploring the designs of bio-bots. *Soft Sci.* **2025**, *5*, 5. https://dx.doi.org/10.20517/ss.2024.50

Received: 8 Oct 2024 **First Decision:** 28 Oct 2024 **Revised:** 27 Nov 2024 **Accepted:** 4 Dec 2024 **Published:** 17 Jan 2025

Academic Editor: Zhigang Wu **Copy Editor:** Ting-Ting Hu **Production Editor:** Ting-Ting Hu

Abstract

Biohybrid robots (bio-bots), made of biocompatible skeletons with living drives (e.g., biological living tissues or cells), represent a new direction of robotics technology due to their attractive advantages of softness, flexibility, adaptability and biocompatibility, accompanied by the remarkable capabilities of self-assembly, self-healing, and self-replication. This paper provides a brief review of recent advances of bio-bots from a functional view, including walking, swimming and non-locomotion bio-bots, by exploring their structure designs along with their operational principles. The performances of these bio-bots are summarized and compared followed by the discussions of challenges and perspectives, which provide valuable insight and guidance for future developments of bio-bots.

Keywords: Biohybrid robot, bio-bot, robotics technology, structure design, living drive

INTRODUCTION

Robotics technology has been developing rapidly in the past few decades with increasing interest from traditional rigid robots to new forms of robots such as soft robots and biohybrid robots (Bio-bots). Traditional rigid robots, usually made of metal or tough materials with rigid drives (e.g., motors or gas

engines), offer advantages of strong load-bearing capacity[1-4], high operating accuracy[5-8] and good stability[9-16], and have benefited humans in many repetitive and heavy tasks. The lack of flexibility in rigid robots limits their application scenarios and adaptions to complex environments. Soft robots, made of flexible materials with soft drives (e.g., stimuli-active materials such as dielectric elastomers[17-21], shape memory polymers[22-25], liquid crystal elastomers[26-29], *etc.*), offer advantages of light weight, strong deformability and good environmental adaptability, and provide a convincing solution to resolve the flexibility challenge of rigid robots as demonstrated in developing flying soft robots[30,31], swimming soft robots[32-34], jumping soft robots[35,36], crawling soft robots[37-39], *etc.* Despite these notable advances in soft robots, soft drives based on stimuli-active materials still have certain disadvantages such as high driving voltage, high driving temperature, low power density and poor biocompatibility, which greatly hinder their practical utilities, particularly in the fields of biomedicine and organ-on-a-chip system.

With the development of tissue engineering and three-dimensional (3D) printing of biomaterials, bio-bots, made of biocompatible skeletons with living drives (e.g., biological living tissues or cells), become a promising solution for expanding the application scenarios of exiting rigid and soft robots. In bio-bots, biological tissues or cells serve as drives to deform the biocompatible scaffolds to achieve desired functionalities (e.g., walking, swimming, *etc.*), which are similar to the skeletal-muscle system of organisms. Compared to nonliving rigid and soft robots, bio-bots possess the advantages of softness, flexibility, adaptability and biocompatibility, accompanied by the remarkable capabilities[40-44] of self-assembly, self-healing, and self-replication. For example, the self-healing property of skeletal muscle was demonstrated to repair mechanical damage[44]. Furthermore, bio-bots can operate entirely through non-contact stimulation with a high-power density due to their unique energy source: living cells primarily utilize nutrient solution (e.g., glucose), which provides Adenosine triphosphate (ATP) required for cell activities, ensuring high energy conversion efficiency[45]. These advancements herald a new era in robotics, offering unprecedented potential for applications in fields ranging from healthcare to environmental monitoring.

A research boom of bio-bots has been seen over the past ten years. Although there exist several reviews of bio-bots focusing on materials and applications, this paper reviews the advances of bio-bots from a functional view by exploring their structure designs. Fundamentals of design principles for bio-bots are first presented. Next, comprehensive overviews of the up-to-date developments of bio-bots, which are classified into walking, swimming and non-locomotion bio-bots (e.g., pump, tweezer, *etc.*), are provided with a focus on the structure design, functional mechanism, and functional performance. Finally, perspectives and challenges are discussed, providing guidance for future developments and performance improvements of bio-bots.

FUNDAMENTALS OF DESIGN PRINCIPLES FOR BIO-BOTS

Bio-bots are mainly made of biocompatible materials serving as skeletons and biological living tissues or cells serving as drives. Living tissues and cells can be stimulated electrically or optically to cause contraction, resulting from the process of excitation-contraction coupling. The electrical stimulation, which is usually generated by placing a pair of parallel electrode rods or sheets into the electrolyte solution or drive, mimics natural neural signals, triggering an action potential that prompts the release of calcium ions from the sarcoplasmic reticulum. These ions bind to troponin and cause a conformational change in actin and myosin filaments, which enables cross-bridge formation and muscle contraction. For the optically stimulated muscle contraction, optogenetic modification is used to introduce genes encoding light-sensitive ion channels, such as Channelrhodopsin-2 (ChR2), into muscle cells. Exposure to specific light wavelengths opens these channels, allowing ion influx that generates an action potential and activates excitation-contraction coupling, resulting in muscle contraction. As a result, the drives supply energy to deform the

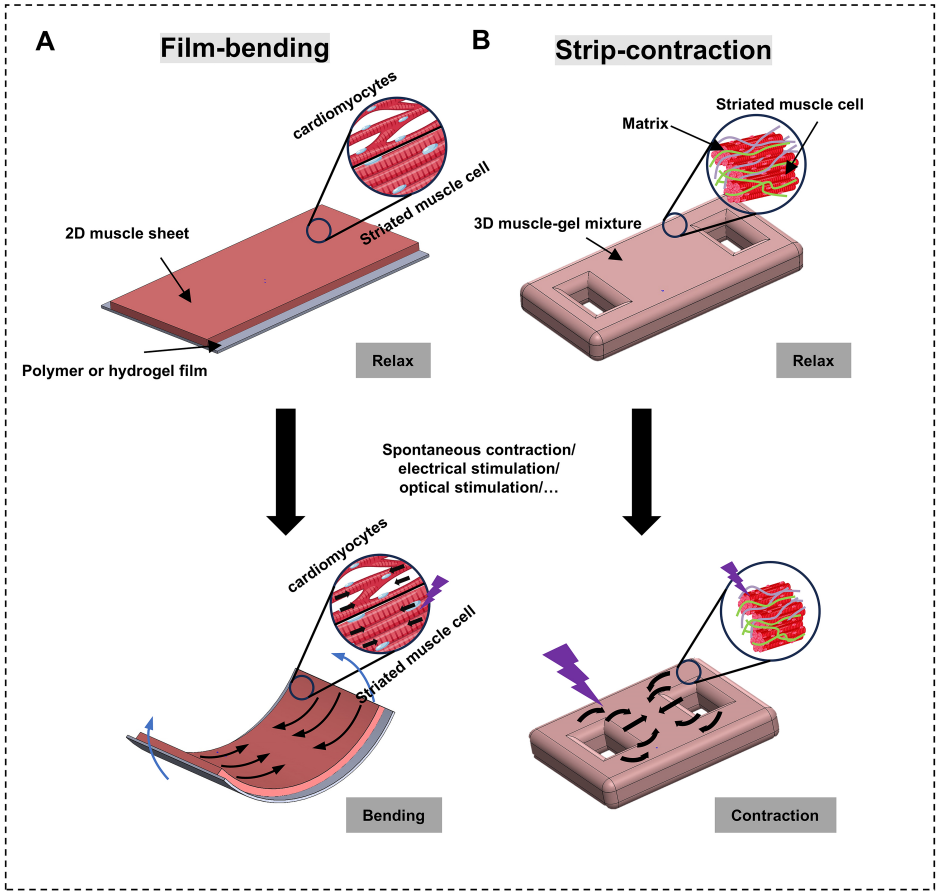

Figure 1. The driving principles of bio-bots powered by living cells: (A) film-bending and (B) strip-contraction.

scaffolds, enabling functions such as walking, swimming or other desired functions, with efficiency greatly depending on the structural design. Based on the driving principles of living drives, the bio-bots can be classified as film-bending- and strip-contraction-based bio-bots with their design principles schematically demonstrated in Figure 1.

The film-bending-based bio-bots adopt a film-shaped drive [Figure 1A], which features cardiomyocytes or striated muscle cells on an ultra-thin hydrogel or polymer film based on two-dimensional (2D) culture of muscle cells. The spontaneous or stimuli-actuated contractions of living cells yield a strain mismatch between the cell layer and the film layer, which causes the film-shaped drive to bend, thus providing a driving force for bio-bots. The assembly of the film-shaped drive with hydrogel or polymer skeletons yields the film-bending-based bio-bots with desired functionalities. With the rapid development of tissue engineering, extracellular matrices (such as matrigel, collagen, *etc.*) can connect cells together to form 3D tissues and organs[46-56], i.e., the strip-shaped drive, offering more ways to construct complex bio-bots by controlling the cell growth, shape and metabolism. The strip-contraction-based bio-bots adopt a muscle-like strip-shaped drive [Figure 1B], which features the mixture of extracellular matrix with muscle cells. The spontaneous or stimuli-actuated contractions of living cells yield a contraction of the strip-shaped drive directly to provide a driving force for bio-bots. It should be noted that the strip-shaped drive utilizes its overall volume contraction and expansion without the need of a pre-stretch. By assembling the strip-shaped drive with hydrogel or polymer skeletons, a strip-contraction-based bio-bot that performs specific functions can be achieved. With the above two driving principles, various bio-bots with different functions have been

demonstrated. Based on the functionalities, bio-bots can be classified into three categories: walking, swimming and other non-locomotion bio-bots (e.g., micropump, microtweezer, *etc.*), as illustrated in Figure 2.

WALKING BIO-BOTS

Walking bio-bots are a very representative type of moving bio-bots. Their movement postures are often imitated by insects and reptiles in nature. A big challenge in designing walking bio-bots is how to overcome the friction between the bio-bots and the plane of motion.

Film-bending-based walking bio-bots

Film-bending-based walking bio-bots primarily employ the design of muscle tissue layers integrated with membranes. This design circumvents the use of complex hinges, which are challenging to manufacture, and provides an easy way to control the locomotion of bio-bots. Currently, bio-bots emulating inchworms[57-59], crabs[60], snakes[61], and caterpillars[62] have emerged. Despite their diverse appearances, they share a common underlying principle: converting the force generated by muscle tissue contraction into asymmetric frictional forces. These frictional forces must exceed the resistance encountered by the bio-bot to enable its directed crawling motion.

To generate asymmetric frictional forces, a common approach involves designing an asymmetric overall structure. One of the earliest demonstrations of film-bending-based walking bio-bots was the inchworm-like bio-bot [Figure 3A], which was developed by Xi *et al.* in 2005. The bio-bot was driven by the contraction of cardiomyocyte bundles and could achieve a speed of up to 38 μm/s[57]. The asymmetry in structure, realized via the integration of muscle tissue with a membrane followed by folding or manufacturing the membrane into asymmetric spatial configurations, leads to unequal frictional forces between the front feet/substrate and the rear feet/substrate contact surfaces during each cycle of muscle contraction and relaxation, resulting in asymmetric displacement and facilitating forward stepping motion. As schematically illustrated in Figure 3A (i), the inchworm-like bio-bot consists of legs made of Cr/Au thin films and a silicon anchor beam, with each leg designed to have a foot to increase the contact area between the leg and the substrate. The Cr/Au film not only adjusts the shape of cardiomyocyte bundles but also stores energy during bending, aiding in the relaxation process. The anchor beam restricts the bending of the rear leg, minimizing its contribution to motion during cardiac muscle contraction, while the bending of the front leg propels the bio-bot forward. During muscle relaxation, the frictional balance between the front and rear legs prevents significant forward or backward movement of the bio-bot, enabling it to advance during the contraction-release process of muscle tissue, as depicted in Figure 3A (ii).

Similar to the motion of the inchworm-like bio-bot, Feinberg *et al.* cultured a type of 2D muscular thin films and designed a series of bio-bots by folding the membrane to create spatial configurations, including a myopod-like bio-bot driven by autonomous contraction of cardiomyocytes or electrical stimulation[58]. The myopod was fabricated from muscular thin films with isotropic 2D myocardium, thereby disrupting the symmetry of frictional forces through the design of asymmetric spatial structures. The structure involved folding one corner of the triangular muscular thin films to form two parts: the rear leg and the angled footpad. As shown in Figure 3B, with the contraction of cardiomyocytes, the rear leg extended and pushed the footpad forward. Conversely, during muscle relaxation, the angled footpad remained stationary, preventing backward slipping of the myopod. Through continuous contraction and relaxation, the myopod-like bio-bot could walk along the bottom of a Petri dish in a directed path under spontaneous or paced contractions with a constant speed of 8 mm/min. Similarly, Chan *et al.* also proposed a bio-bot consisting of a "biological bimorph" cantilever structure as the actuator to power the bio-bot with a max velocity of

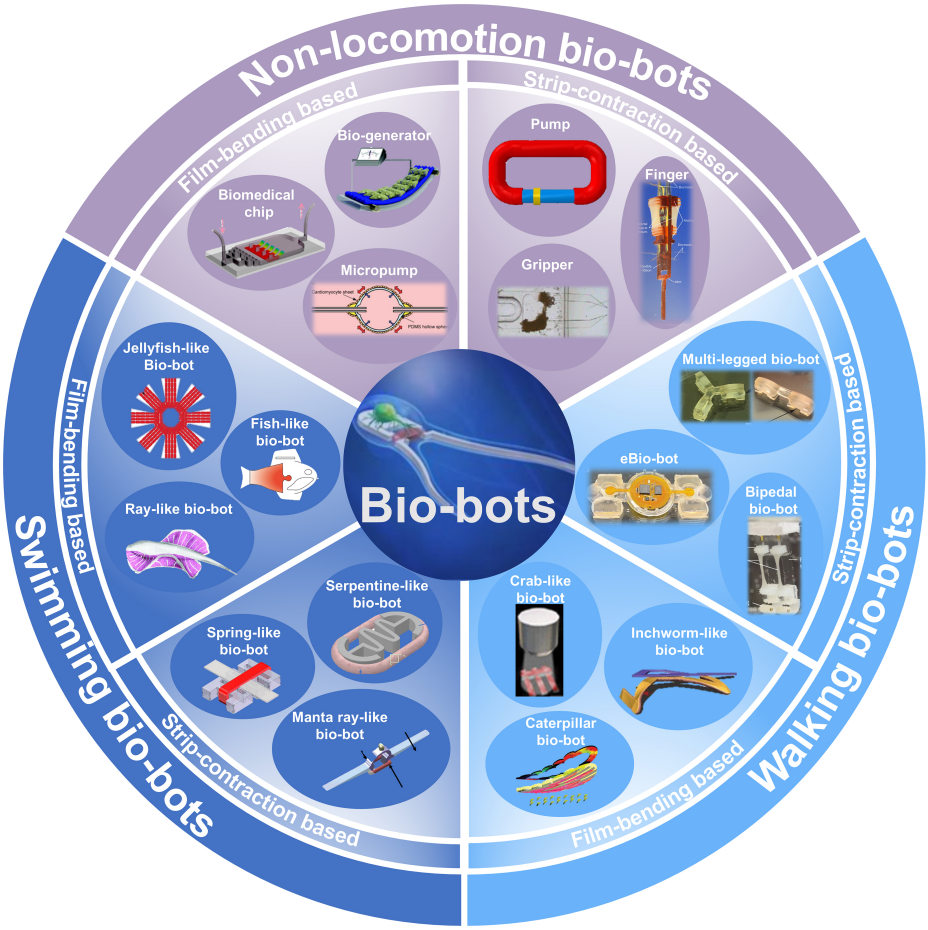

Figure 2. Overview of bio-bots, including walking, swimming and non-locomotion bio-bots. Reproduced with permissions[57]. Copyright 2005, Springer Nature. Reproduced with permission[60]. Copyright 2007, RSC. Reproduced with permission[62]. Copyright 2018, WILEY VCH. Reproduced with permission[64]. Copyright 2023, The American Association for the Advancement of Science. Reproduced with permission[65]. Copyright 2022, Wang *et al.* Reproduced with permission[66]. Copyright 2023, Elsevier. Reproduced with permission[70]. Copyright 2012, Springer Nature. Reproduced with permission[72]. Copyright 2016, The American Association for the Advancement of Science. Reproduced with permission[73]. Copyright 2022, The American Association for the Advancement of Science. Reproduced with permission[77]. Copyright 2019, Aydin *et al.* Reproduced with permission[79]. Copyright 2022, Zhang *et al.* Reproduced with permission[81]. Copyright 2021, American Association for the Advancement of Science. Reproduced with permission[80]. Copyright 2024, Zhongguo Kexue Zazhishe. Reproduced with permission[86]. Copyright 2007, RSC. Reproduced with permission[91]. Copyright 2016, RSC. Reproduced with permission[92]. Copyright 2018, American Association for the Advancement of Science. Reproduced with permission[88]. Copyright 2019, Li *et al.* Reproduced with permission[94]. Copyright 2013, RSC. Reproduced with permission[96]. Copyright 2018, American Association for the Advancement of Science.

236 μm/s[59].

In order to achieve long-term monitoring of primary cultured cardiomyocytes on microscale robots, Kim *et al.* introduced a crab-like bio-bot driven by the spontaneous contraction of cardiomyocytes[60]. Its asymmetric structure consisted of three connected Polydimethylsiloxane (PDMS) membranes, subdivided into three legs of 400 μm in length for the front legs and 1,200 μm for the rear legs. The multiple legs were attached to the middle of the robot body, enabling synchronous contraction by connecting with cardiomyocytes. To enhance the concentration of cardiomyocyte force, a grooved pattern was engraved on the surface of the legs, facilitating the crab-like bio-bot to achieve directed motion at an average velocity of approximately 100 μm/s. As depicted in Figure 3C, during locomotion, the longer legs bent inward more,

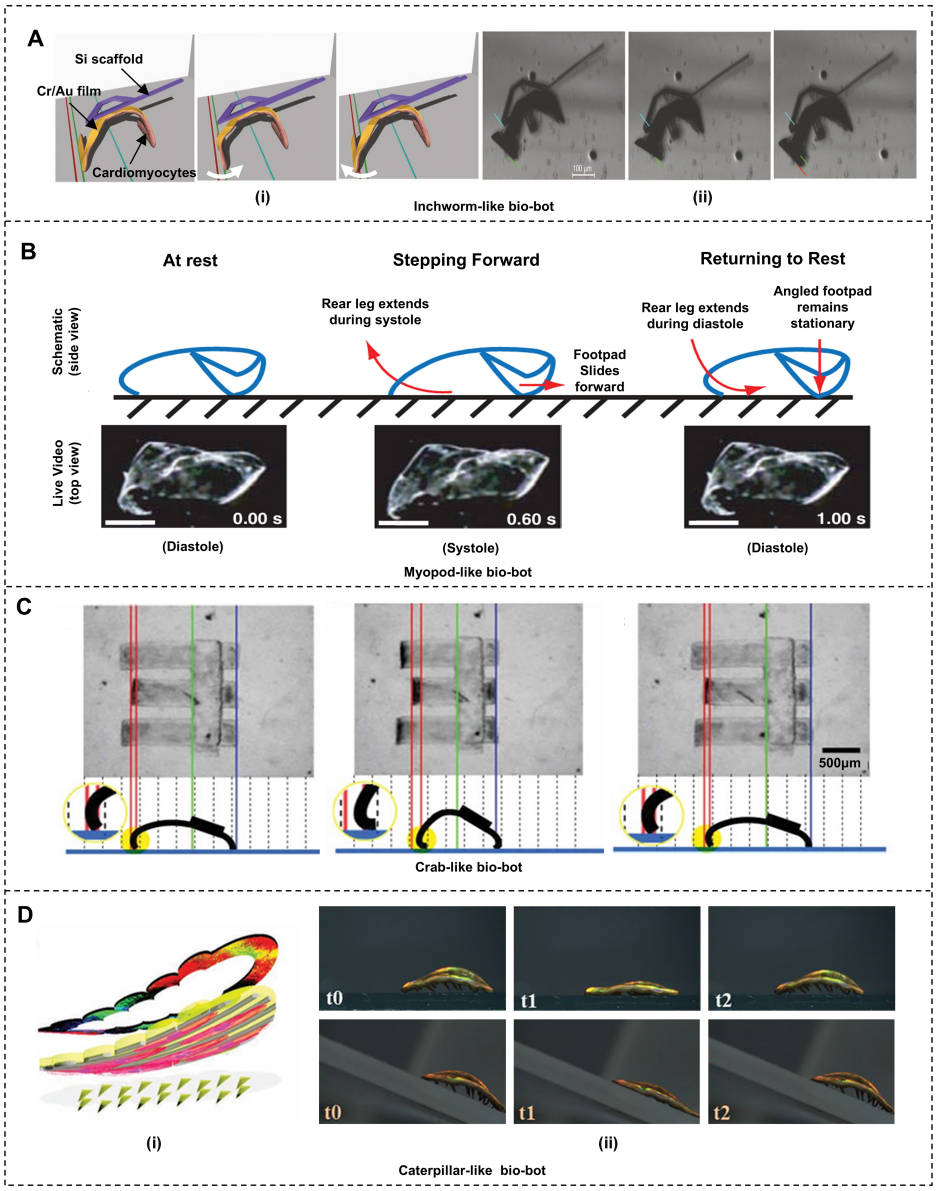

Figure 3. Film-bending-based walking bio-bots. (A) An inchworm-like bio-bot moved forward. The sequential movement of the bio-bot shown by (i). schematic diagrams and (ii). microscope images. Reproduced with permission[57]. Copyright 2005, Springer Nature; (B) A myopod-like bio-bot capable of autonomous or remote-controlled walking. Reproduced with permission[58]. Copyright 2007, The American Association for the Advancement of Science; (C) A crab-like bio-bot designed as an asymmetric structure with three front and rear legs of different lengths showing the sequential movement during one step. Reproduced with permission[60]. Copyright 2007, RSC; (D) A caterpillar-like bio-bot that causes asymmetrical friction through a designed microstructure on the underside. (i). The structure of the caterpillar-like bio-bot; (ii). The crawling process of bio-bot on an incline of 10°. Reproduced with permission[62]. Copyright 2018, WILEY VCH.

causing the outside PDMS of the longer legs to contact the bottom surface, inducing frictional differences between legs and propelling the robot towards the side with shorter legs. Long-term monitoring demonstrated that the crab-like bio-bot could maintain activity for extended periods in suitable culture conditions and continuously move for 7 days.

Inspired by the crawling mechanisms of caterpillars, Sun *et al.* developed a bio-bot driven by cardiomyocytes, featuring biomimetic microstructural characteristics[62]. As shown in Figure 3D (i), the caterpillar-like bio-bot consisted of snake-skin-like claws, a parallel carbon nanotube (CNT)-assisted myocardial tissue layer, and a structural color indicator layer. Drawing inspiration from the ventral scales of snakes, asymmetric claws with inclined angles were designed at the bottom to achieve frictional anisotropy, thereby enabling the directed locomotion function of the bio-bot. As illustrated in Figure 3D (ii), the caterpillar-like bio-bot achieved motion at approximately 20 μm/s on a rough substrate and could crawl on a substrate inclined at 20°. Notably, a structural color layer was introduced in the caterpillar-like bio-bot, allowing for reversible color changes during deformation to visualize the contraction of cardiac muscle and the motion state of the robot.

Strip-contraction-based walking bio-bots

Compared to structurally simpler film-bending-based walking bio-bots, strip-contraction-based walking bio-bots are more worthy of investigation. They possess the capability for multidimensional movement, enabling them to maneuver freely in space, including crawling[63-69] and other movements. This allows these robots to respond to more complex environments and tasks.

To improve the low controllability in the motion of bio-bots, Zhang *et al.* designed a biped bio-bot[63]. As shown in Figure 4A (i), asymmetric structures made of PDMS serve as the robot's feet. The motion of each foot determines the overall motion speed and direction of the robot, propelled by controllable muscular rings assembled on them. By electrically stimulating the contraction of muscle tissue, the feet of the robot with elastic structures are induced to generate motion. Placing the biped robot under a tunable directional electric field enabled highly controllable manipulation of its motion speed and direction. This involves modulating the contractility of muscle tissues by altering the stimulation angle between tissue axial orientation and electric field direction. Furthermore, a circular distributed multiple-electrode remote control system was developed to dynamically generate and control electric stimulation in any direction by adjusting the electric potential of each electrode. This enables selective stimulation of muscle tissues on the robot's feet to induce contraction in different directions. Based on the response characteristics of the single-footed robot to electric field direction, the larger the angle between the two feet of the bipedal bio-bot, the better its directional controllability. Additionally, according to the principles of projection geometry, the larger the angle between the two feet, the lower the motion efficiency. To balance the controllability and motion speed of the bipedal robot, the angle between the two feet was designed as 60°. To validate the manipulability of the bipedal robot's motion, the robot was placed in the circular distributed multiple-electrode remote control system, and different-directional electric pulses with an amplitude of 2 V/cm, frequency of 2 Hz, and width of 20 ms were utilized to stimulate the bipedal robot's walking. As illustrated in Figure 4A (ii), the results indicate that, with a biped angle of 60°, the robot can achieve overall motion behaviors including straight walking, right turn, and left turn with a turning range of 12.563°, and an average angular velocity of 0.3152 °/s.

To further improve the controllability of bio-bots, Kim *et al.* employed a wireless optoelectronic technology for controlling optogenetics-driven skeletal muscle-based biped biohybrid electronic robots (ebio-bots)[64], enabling remote control for switching, steering, and other complex functionalities. Figure 4B (i) shows a single-legged ebio-bot, which features 3D-engineered skeletal muscle tissue forming around an asymmetric hydrogel scaffold and wireless optogenetic device assembled onto the framework. The muscles respond to external light stimulation and undergo cyclic contractions, driving the locomotion of the robot through asymmetric friction generated at the scaffold-matrix interface. When stimulated by pulses of the frequency of 4 Hz, the pulse width of 50 ms and the power of 10 W, the maximum walking speed of the single-legged walking robot could reach 0.83 mm/s. To further enhance the robot's maneuverability and accomplish

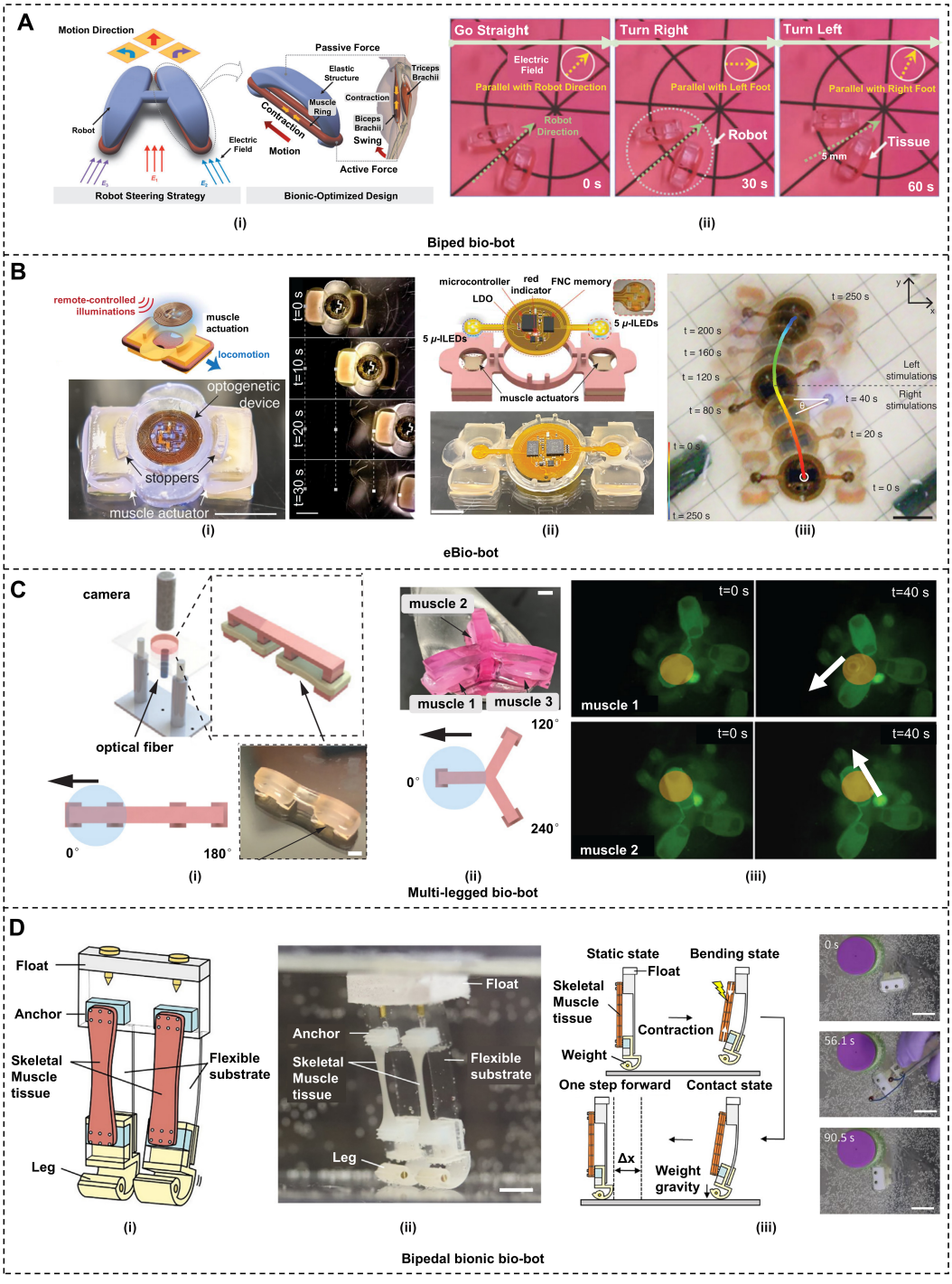

Figure 4. Strip-contraction-based walking bio-bots. (A) A biped bio-bot. (i) Design principle and schematic diagram of the biped bio-bot; (ii) Control of biped bio-bot locomotion by electrical stimulation in different directions. Reproduced with permission[63]. Copyright 2024, Mary Ann Liebert, Inc; (B) Remote light-controlled muscle-driven eBio-bot. (i) Design and movement of the single actuator eBio-bot; (ii) The structure composition of biped eBio-bot; (iii) Trajectory and time-lapse images of bidirectional-turning of eBiobot. Reproduced with permission[64]. Copyright 2023, The American Association for the Advancement of Science; (C) Light-controlled multi-legged bio-bots for (i) bi-directional and (ii) tri-directional walking. Reproduced with permission[65]. Copyright 2022, Wang *et al.*; (D) A bipedal bionic bio-bot with two legs. (i) Concept and optical image of the bipedal bionic bio-bot powered by cultured skeletal muscle tissue; (ii) Principle of movement of the bipedal bionic bio-bot; (iii) Lifting and stepping out distances of the bipedal robot during one cycle of locomotion. Reproduced with permission[66]. Copyright 2023, Elsevier.

complex motions, inspired by bipedal structures and biological locomotion units, Kim *et al.* designed a bipedal ebio-bot, which features two skeletal muscle actuators and a central microcontroller[64] [Figure 4B (ii)]. Symmetric (both at 4 Hz) or differential (4 and 1 Hz) stimulation schemes can be applied for two muscles to achieve complex functionalities such as straight walking and bidirectional turning in the bipedal robot. By alternating the stimulation frequency between the two legs, as depicted in Figure 4B (iii), the bipedal eBio-bot's ability to execute bidirectional turning under remote control during a continuous run was validated.

In addition to the bipedal structure design, Wang *et al.* also proposed a multi-legged design concept[65] by injecting a mixture of myoblasts and matrix into the multi-pillar mold, allowing the muscle tissue to grow and mature on the hydrogel multi-legged structure. This resulted in the fabrication of multi-legged bio-bots capable of bidirectional or multidirectional walking responses to non-invasive optical stimulation. As illustrated in Figure 4C (i), to achieve unidirectional motion, asymmetric designs are utilized, serially connecting two asymmetric robots to form an overall symmetric bio-bot. Stimulation with 4Hz light enables bidirectional walking at a speed of up to 13 mm/min. In addition to bidirectional motion, more complex geometric shapes have also been explored. The tri-directional bio-bot with three independent muscle actuators uniformly walks in three directions, with speeds ranging from 1 to 4 mm/min. As shown in Figure 4C (ii), when muscle 1 is stimulated by optic, the bio-bot walks in the direction of muscle 1, and when muscle 2 is stimulated, the bio-bot walks in the direction of muscle 2. These multi-legged bio-bots expand the degrees of freedom of the walking hybrid robot, making turning movements easier to achieve.

Recently, inspired by the structure and behavior of human bipedal locomotion, Kinjo *et al.* proposed a bipedal bionic bio-bot powered by cultured skeletal muscle tissue with capabilities of forward and stop motions and fine turning movements[66]. As illustrated in Figure 4D (i), the bipedal bionic bio-bot capable of maintaining an upright posture consists of a float, a body made of PDMS with two flexible substrates, 3D-printed legs, and cultured skeletal muscle tissues. As depicted in Figure 4D (ii), when the cultured skeletal muscle tissue contracts in response to electrical stimulation, the flexible base of the leg noticeably bends from its initial state, effectively becoming a pivot leg. Subsequently, the heel of this leg contacts the bottom surface of an acrylic square container as the skeletal muscle tissue relaxes, causing a partial forward movement of the body aided by the elasticity of the substrate. Based on this principle of motion, when appropriate electrical stimulation is applied to the cultured skeletal muscle tissue on either the left or right side, the robot can move forward. As shown in Figure 4D (iii), the two legs of the bipedal bionic bio-bot anchor ground contact points through the weight of the legs to provide a physical pivot center, enabling it to perform compact turns. When the right leg contracts due to electrical stimulation, the robot turns left. Within 90.5 s, the robot completes a 90-degree turn, with electrical stimulation applied every 5 s, resulting in an angular velocity of 1.4 °/s. The unstimulated left leg acts as the axial support during the turning process, maintaining relative stability. It can be considered that this bipedal bionic bio-bot is closest to human gait at present.

SWIMMING BIO-BOTS

Swimming bio-bots are another representative type of moving bio-bots. The design of swimming bio-bots is usually inspired by various aquatic organisms in nature, from microorganisms in the water to various fish organisms. By mimicking the swimming of these creatures, many swimming bio-bots have been designed[58,70-84].

Film-bending-based swimming bio-bots

By analyzing the structure and movement of jellyfish in nature, Nawroth *et al.* reported a jellyfish-like swimming bio-bot, termed "medusoid", using neonatal rat cardiomyocytes and silicone polymer (PDMS) thin film[70]. Similar to the physiology of jellyfish, fast contraction of cardiomyocytes and slow recoil of elastomer constituted asymmetric stroke patterns, resulting in propulsion [Figure 5A (i)]. In order to control the contraction frequency of cardiomyocytes and the movement of jellyfish-like swimming bio-bots, electrical stimulation was applied to activate contraction. Figure 5A (ii) demonstrates a complete process of stroke: medusoid started in a resting state (t = 0), then the cardiomyocytes contracted (t = 0.3T. T = stroke cycle) followed by the recoil of the elastomer (t = 0.6T). The motion performance of medusoid mostly ranged between 0.4 and 0.7 body lengths traveled per swimming stroke (BL/S). To further simplify the structure, instead of using a two-layered structure, Takemura *et al.* reported a jellyfish-like robot consisting solely of cardiomyocytes gel, fabricated by mixing cardiomyocytes with collagen gel[71]. It could move along the bottom of a petri dish at an average speed of 6.9 μm/s due to the differences in pulsation displacement between points on the body's edge. The study also revealed that the pulse frequency and moving velocity of the bio-bot could be controlled through chemical stimulation using epinephrine or nifedipine.

In 2007, Feinberg *et al.* demonstrated a triangular swimming bio-bot as shown in Figure 5B[58]. The triangle swimmer consisted of a triangular PDMS thin film and cardiomyocytes aligned along blue lines. Thus, when the cardiomyocytes contracted, the film bent in the direction indicated by the red arrow [Figure 5B (i)]. Figure 5B (ii) demonstrates a similar process of motion: a relaxed construct, followed by contraction, recoiling to produce propulsion, and finally returning to the original shape, allowing the bio-bot to swim. The swimming bio-bot revealed a maximum swimming velocity of ~ 24 mm/min at 1 Hz pacing.

In 2015, inspired by batoid fishlike stingrays and skates, Park *et al.* created a biohybrid batoid fish capable of phototactically following a light cue, which is only 1/10 scale of the real batoid fish[72]. The serpentine-patterned cardiomyocyte circuits and a stiff gold skeleton induced sequential muscle activation under optical stimulation, leading to chordwise front-to-rear undulatory motion and forward propulsion [Figure 5C (i and ii)]. Additionally, the direction of motion could be changed by independently activating the right and left fins [Figure 5C (i)]. The ray-like swimmer demonstrated excellent performance in terms of speed (3.2 mm/s), distance traveled (~ 250 mm), and durability (6 days).

From this, Lee *et al.* then turned their attention to spindle-shaped fish, one of the most common fish species[73]. In 2022, an autonomously swimming biohybrid fish equipped with an antagonistic cardiac muscle pair (i.e., the contraction of one muscle is accompanied by the relaxation of the other) was created, producing coordinated body-caudal fin propulsion [Figure 5D (i)]. The muscular bilayer consisted of two layers of muscle: the left layer was genetically modified to be sensitive to red light, while the right layer was sensitive to blue light, enabling the hybrid fish to swim autonomously or optogenetically [Figure 5D (ii)]. Furthermore, the biohybrid fish, with a speed of 15 mm/s, demonstrated comparable efficiencies to wild-type fish and was capable of maintaining spontaneous activity for 108 days. Shin *et al.* also reported a similar actuator with aligned CNT forest microelectrode arrays embedded into scaffolds for cell stimulation[74]. The actuator could beat as the cardiomyocytes spontaneously contracted and be precisely controlled by applying an external electric field. When the actuator beat, its edges rolled up, but it did not exhibit any locomotion. Similarly, in 2022, Tetsuka *et al.* developed a swimming, remotely controllable bio-bot in which wirelessly powered cell stimulators were integrated into muscle bodies[75]. Additionally, the speed and direction of the robot can also be controlled by wirelessly modulating electrical frequencies, achieving a maximum locomotion speed of 580 μm/s. Inspired by the swimming of whales and light-sensitive materials, Xu *et al.* also developed a remotely controlled, transformable swimming bio-bot based on cardiomyocytes[76]. The swimmer featured a cardiac tail fin to push off the media for driving motion and

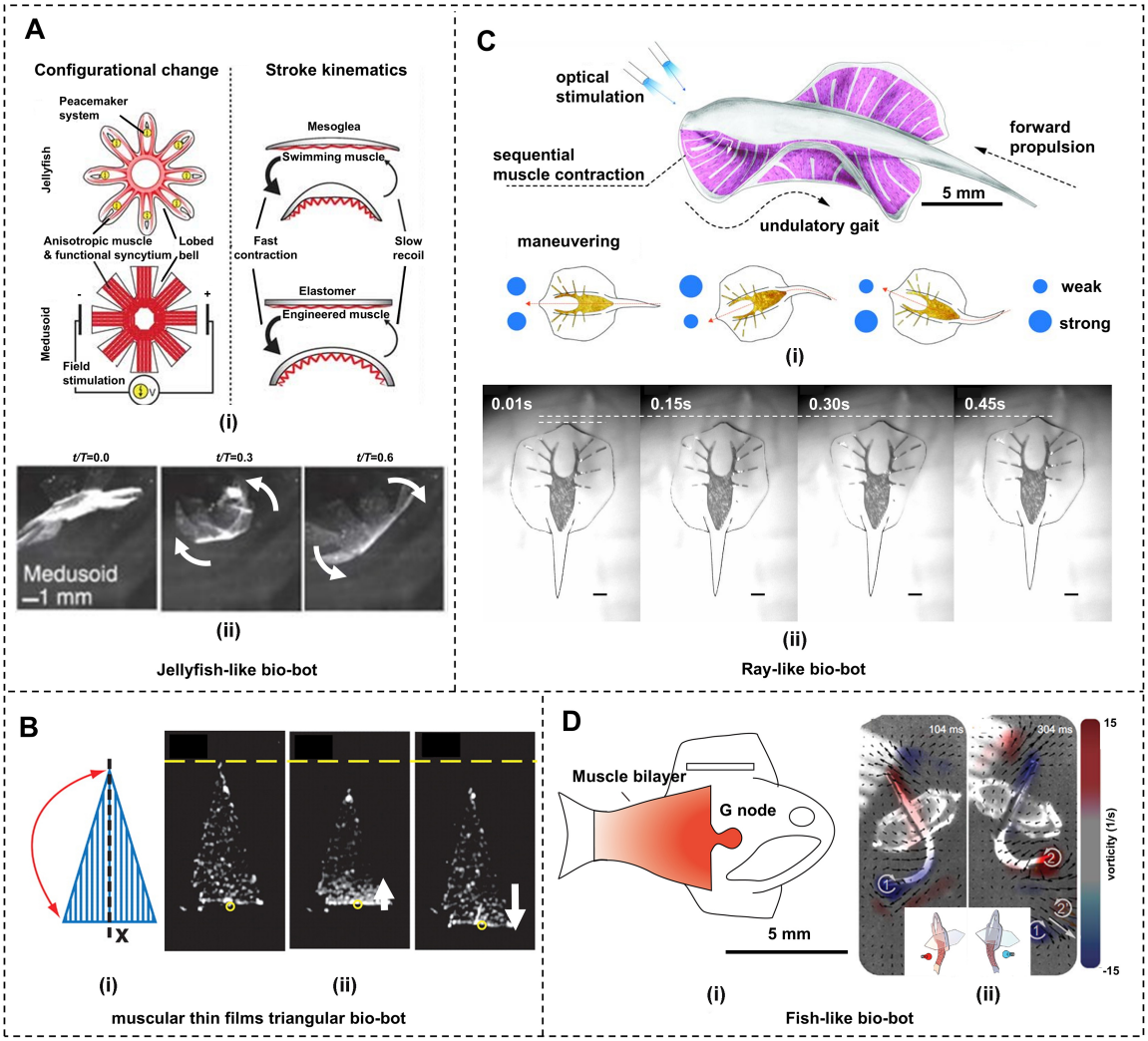

Figure 5. Film-bending-based swimming bio-bots. (A) A jellyfish-like swimming bio-bot driven by cardiomyocytes. (i) Comparison of configuration and stroke kinematics between jellyfish and jellyfish-like swimming bio-bot; (ii) Time-lapse of stroke cycle in jellyfish-like swimming bio-bot. Reproduced with permission[70]. Copyright 2012, Springer Nature America, Inc; (B) A muscular thin films triangular swimmer made of cardiomyocytes. (i) The structure of the swimmer; (ii) Consecutive video frames during motion Reproduced with permission[58]. Copyright 2007, The American Association for the Advancement of Science; (C) A ray-inspired swimming robot capable of undulatory swimming. (i) Concept design of the bio-bot including structure and phototactic control; (ii) optical images of a complete process of undulatory locomotion. Reproduced with permission[72]. Copyright 2016, The American Association for the Advancement of Science; (D) A fish-inspired swimming robot with an antagonistic muscle pair. (i) Structure of the bio-bot; (ii) Optical images when the muscle pair are separately contracted. Reproduced with permission[73]. Copyright 2022, The American Association for the Advancement of Science.

photosensitive wings for transformation. The floating-plane bio-bot had an average moving speed of 0.8 mm/s and could maintain a good state for up to three weeks. When exposed to near-infrared (NIR) light, the photosensitive wings transformed into a nearly cylindrical shape within several seconds upon heating to 37 °C, dramatically increasing the bending stiffness and thereby halting the motion. Upon removal of NIR irradiation, the robot's motion immediately resumed.

Strip-contraction-based swimming bio-bots

Inspired by flagellate, Aydin *et al.* presented a kind of light-sensitive swimmer at low Reynolds numbers which was driven by on-board neuromuscular units consisting of the neuron and the muscle strip[77]

[Figure 6A (i)]. In their study, a single-tailed and a two-tailed swimmer were demonstrated, mimicking the swimming mechanisms of spermatozoa and bacteria, which oscillate or twist a flagellum to propel themselves. When the neuron reacted to 470 nm light and drove the skeletal muscles to contract, the flagella deflected, and a bending wave propagated from the actuation site to the free end of the tail, thereby providing the thrust for the forward locomotion of the swimmer [Figure 6A (ii)]. Given the targeted low Reynolds numbers regime and the viscous drag associated with the voluminous head, the swimming speeds were relatively low, approximately 0.7 μm/s. In 2014, Williams *et al*. reported a similar microscale biohybrid swimmer at a low Reynolds number, which included a PDMS head and tail, with cardiomyocytes cultured in a small section of the tail[78]. For the demonstrated bio-bots, contractions of the cardiomyocytes bent the tail, producing a net thrust that propelled the swimmer forward. The demonstrated single-tailed swimmer and two-tailed swimmer had speeds of 9.7 and 81 μm/s, respectively.

Zhang *et al*. were inspired by manta rays and developed a manta ray-inspired bio-bot[79], as shown in [Figure 6B (i)]. The bio-bot consisted of a deformable PDMS skeleton and two polyimide (PI) fin structures to maintain stability. The skeletal muscle strip was fixed to the structure and pulled to drive the two fin structures to swing. The Bio-bot swims by flapping its fins, similar to a manta ray. Figure 6B (ii) shows the continuous process of the Bio-bot swimming. He *et al*. also tried to build their own bio-bot[80]. Figure 6C (i) shows a spring-like Bio-bot we proposed, which has a PDMS body resembling a spring and protrusions located on one side. A fin structure made of parafilm was used to maintain stability on the liquid. When the muscle strip was activated and contracted by electrical stimulation, the PDMS structure was compressed, and the protrusions bent toward each other. When the muscle strip contracted and relaxed, the bends at the protrusions resembled the hands paddling inwards, allowing the bio-bot to slide forward. The spring-like body allowed the robot to quickly return to its original shape until the next electrical stimulation pulse arrived. As illustrated in Figure 6C (ii), spring-inspired bio-bot swam a distance of 1.32 mm in 1,670 s, with an average speed of 0.8 μm/s.

Guix *et al*. also presented a skeletal muscle-based swimming bio-bot integrated with a serpentine spring skeleton featuring asymmetric stiffness[81] [Figure 6D (i)]. This design of spring allowed for self-stimulation during the cell maturation process to improve the muscle force output. The design of asymmetric stiffness allowed for different deformations Δx_1 and Δx_2 in two sides, resulting in a net displacement of the bio-bot. As a result, the swimmer achieved a maximum velocity of about 800 μm/s [Figure 6D (ii)]. Additionally, two types of motion were demonstrated: directional swimming when the bio-bot was at the liquid-air interface and coasting motion when it was near the bottom surface. Holly *et al*. developed a self-stabilizing swimming bio-bot consisting of a base made from two composite PDMS materials and a thin PDMS cantilever seeded with heart muscle cells[82]. The spontaneous contraction of cardiomyocytes bent the cantilever, which pushed off the media, resulting in the net displacement of the robot and achieving a maximum velocity of 142 μm/s. A unique feature of the bio-bot was that by changing the resting angle of its "fin", the bio-bot could exhibit different propulsion modes and move forward or backward.

NON-LOCOMOTION BIO-BOTS

Besides locomotion (e.g., walking and swimming) functionality, bio-bots can also perform other specific functions such as pumping[85-90], acting as actuators[91], generating power[92], functioning as bio-chips[93], operating as tweezers[94,95], acting as grippers[96,97], *etc*. These bio-bots are usually achieved by exploiting the interaction between tissues and mechanical systems (chambers, mechanical structures, *etc*.). These robots are referred to as non-locomotion bio-bots in this paper and will be overviewed in this section.

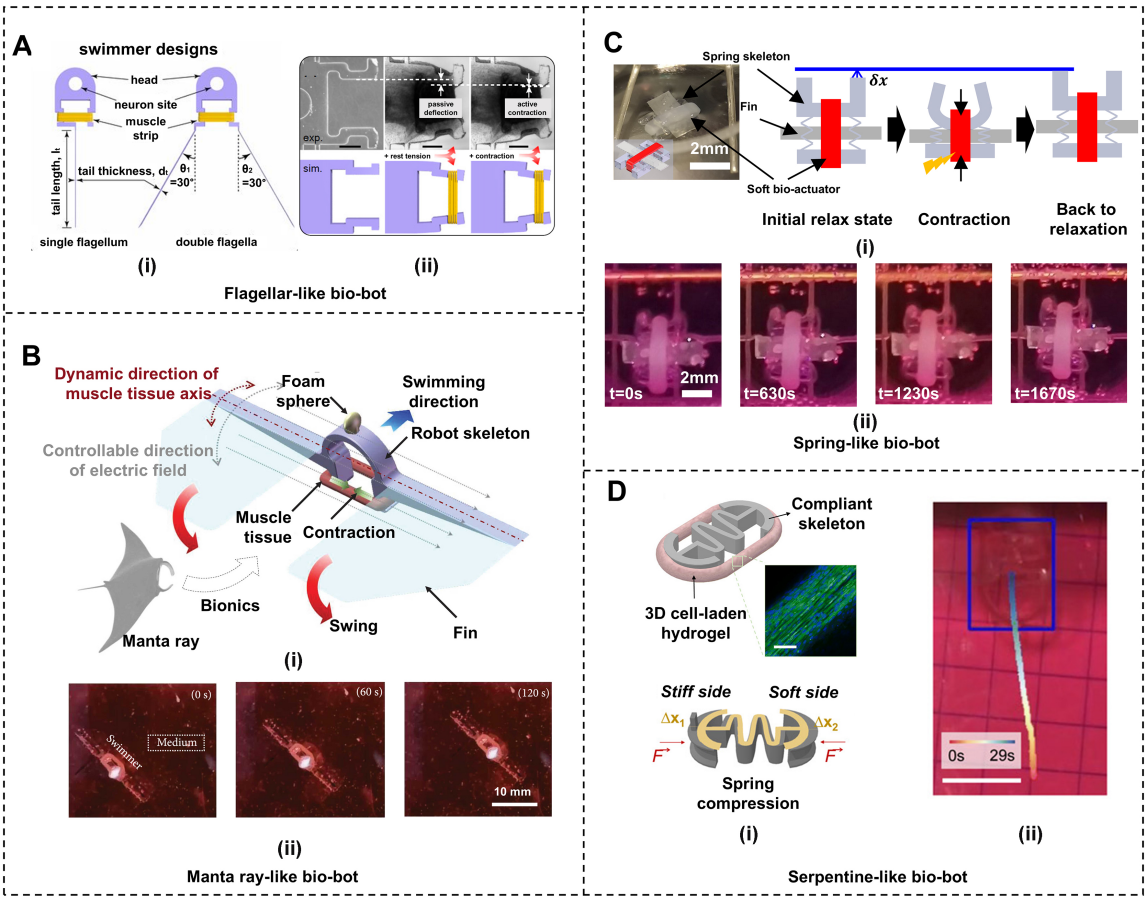

Figure 6. Strip-contraction-based swimming bio-bots. (A) A neuromuscular actuated swimming bio-bot. (i) Configuration of the bio-bot with single flagellum and double flagella, respectively; (ii) Deformation of the scaffold during muscle strip relaxation and contraction. Reproduced with permission[77]. Copyright 2019, Aydin *et al.*; (B) A manta ray-like swimming bio-bot. (i) structure and driving principles of the bio-bot; (ii) Image of the motion trajectory. Reproduced with permission[79]. Copyright 2022, Zhang *et al.*; (C) A spring-like bio-bot. (i) Driving principles of spring-like bio-bot; (ii) Time-lapse images of undulatory locomotion of the bio-bot; (D) A swimming bio-bot with a serpentine skeleton. (i) structure of the bio-bot and the asymmetrical structural stiffness; (ii) Image of the motion trajectory with corresponding distance over time. Reproduced with permission[81]. Copyright 2021, The American Association for the Advancement of Science.

Film-bending-based non-locomotion bio-bots

A typical function of non-locomotion bio-bots is pumping liquid in the field of microfluidics. In 2006, Tanaka *et al.* proposed a cardiomyocytes-driven valved micropump chip that can activate fluid movement in the microchannel[85] [Figure 7A]. The micropump is made of four layers: microchannel layer, chamber layer, check valve layer and cardiomyocytes sheet from bottom to top. When cardiomyocytes contract spontaneously, the cardiomyocyte sheet will be tightened to push the push bar, resulting in increased pressure in the chamber. At the same time, due to the role of the check valve, the liquid can only flow out from the outlet, and is accompanied by the inflow of liquid at the entrance when the cardiomyocytes relax. After repeated contraction of the cardiomyocyte sheet, a directional flow rate of 2 nL/min was produced. The presence of a check valve has a great negative influence on the flow rate. To eliminate this influence and simplify the complex fabrication process, Tanaka *et al.* soon proposed a cardiomyocytes-driven valveless micropump[86]. This micropump is fabricated by wrapping a self-beating cardiomyocyte sheet exhibiting large contractile forces around a fabricated hollow elastomeric sphere (5 mm diameter, 250 μm thickness) fixed with an inlet and outlet, as shown in Figure 7B. When cardiomyocytes contract, the hollow elastomeric sphere is compressed, causing the internal pressure to decrease, and pushes the liquid out of the

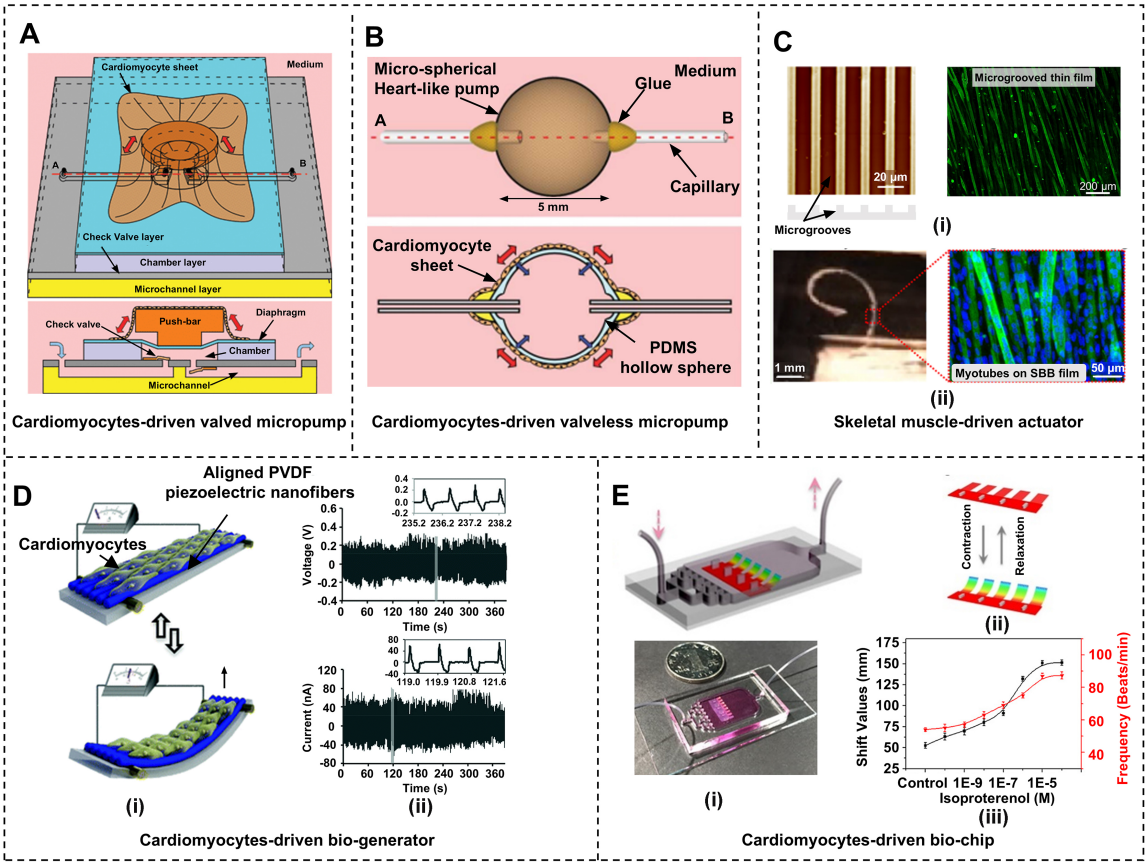

Figure 7. Film-bending-based non-locomotion bio-bots. (A) Schematic diagram of a cardiomyocytes-driven valved micropump. Reproduced with permission[85]. Copyright 2006, RSC; (B) Schematic diagram of the cardiomyocytes-driven valveless micropump. Reproduced with permission[86]. Copyright 2007, RSC; (C) A skeletal muscle-driven actuator. (i) Microscopic image of the microgrooved thin SBS film, causing the skeletal muscle fibers cultured on it to grow along the grooves; (ii) Optical image of the contraction of microgrooved SBS film powered by differentiated myotubes. Reproduced with permission[91]. Copyright 2019, ACS; (D) A cardiomyocytes-driven electric bio-generator. (i) Schematic overview of the cardiomyocytes-driven bio-generator; (ii) Open-circuit voltage signal achieved by the bio-generator. Reproduced with permission[92]. Copyright 2016, RSC; (E) A cardiomyocytes-driven bio-chip for biological research and drug screening. (i) Schematic of the construction of the bio-chip and the bent-up process driven by cardiomyocytes; (ii) Photograph of the bio-chip; (iii) Relationships of the average peak shift values (left) and the beating frequency (right) to the bio-chip with different concentrations of isoproterenol. Reproduced with permission[93]. Copyright 2018, American Association for the Advancement of Science.

chamber. Fluid oscillation in a capillary connected to a hollow sphere induced by the synchronously beating cardiomyocyte sheet was observed. 0.047 μL/min flow rate for the valveless micropump was produced. These kinds of micropumps can be applied for various purposes including medical implant devices that rely on biochemical energy, but not electrical interfacing.

In addition to pumping, actuators with a 2D skeletal muscle sheet structure have also been extensively studied. To achieve a relatively strong contraction, skeletal muscle usually requires a more consistent distribution of muscle fibers. Hasebe *et al.* cultured skeletal muscle cells (C2C12) directly on microgrooved Poly(styrene-blockbutadiene-block-styrene) (SBS) film[91]. Due to the existence of microgrooves on the film [Figure 7C (i)], similar to the microstructure of muscle extracellular matrix, it is conducive to the arrangement and differentiation of skeletal muscle cells. Under electrical stimulation, the SBS film is contracted and curled by skeletal muscle, as shown in Figure 7C (ii). This idea of growing muscle cells on microgrooved thin films could provide the basis for the design of more bio-hybrid actuators in the future.

With the aid of the 2D muscle sheet, in 2016, Liu *et al.* developed a cardiomyocytes-driven bio-generator that can generate electricity[92]. Cardiomyocytes were cultured on fibronectin-coated electrospun Polyvinylidene fluoride (PVDF) nanofibers with uniaxial alignment. The nanofibers can be easily stretched, causing the film to bend, and the fiber structure can also be used as a scaffold for the growth of cardiomyocytes. Figure 7D (i) shows the schematic overview of the conversion of mechanical energy from cardiomyocyte contraction into electrical energy. The cardiomyocytes interact with the flexible nanostructures. The nanofibers guide the growth and contraction direction of the cardiomyocytes. The spontaneous contraction of the cardiomyocytes causes the piezoelectric film to deform and bend to generate electrical energy. Figure 7D (ii) shows the open-circuit voltage signal and current achieved by the bio-generator. The bio-generator produces an average voltage of 200 mV and an average current output of 45 nA at 1.1 Hz frequency, offering a platform for biological energy conversion.

With the introduction of smart material films, some bio-chips are designed and proposed. Fu *et al.* proposed a cardiomyocytes-driven bio-chip composed of a microfluidic channel and a biohybrid structural color hydrogel film[93]. Engineered cardiomyocytes were cultured on the synthetic inverse opal hydrogel films, and a kind of structural color material with self-regulatory ability was constructed. This bio-chip consists of bifurcated injection channels, which provide a uniform culture medium or drugs to the cardiomyocytes, and a patterned structural color hydrogel film with cardiomyocytes growing on it, as shown in Figure 7E (i) The cardiomyocytes repeatedly contract and relax, resulting in the contraction and bending of the hydrogel film [Figure 7E (ii)], which can be observed through the synchronous movement of its photonic band gap and structural color. Due to the structural color of the material varying with different bending degrees, and the position of the reflection peak exhibiting different contractility to the cardiomyocytes, the bio-chip can serve as a functional platform to study the cell behavior of cardiomyocytes and tissues under various conditions. To verify this function, different concentrations of isoproterenol were pumped into the chip to affect cardiomyocytes. When the drug was not added, due to the spontaneous contraction of cardiomyocytes, the structural color of the film changed from red to green, and the reflection peak only experienced a blue shift of about 50 nm. After the addition of isoproterenol, the structural color changes to blue, resulting in a blue shift of about 130 nm. With the increase of the isoproterenol concentration, the change degree of structure color is deepened, and the blue shift of reflection peak is further increased, as shown in Figure 7E (iii). The beating rate of the cardiomyocytes also increases. This example shows that this bio-chip can be used as a biomimetic microphysiological platform for visual biological research and drug screening.

Strip-contraction-based non-locomotion bio-bots

Similar to the micropump enabled by the film-bending-based non-locomotion bio-bots, strip-contraction-based non-locomotion bio-bots have also been widely used in microfluidics, cardiovascular pumping systems, and biomedical equipment. In 2019, Li *et al.* proposed a valveless micropump composed of circular skeletal muscle strips wrapped around a soft hydrogel tube to achieve unidirectional pumping of liquids[88]. Figure 8A (i and ii) shows the schematic diagram and photograph of this skeletal muscle-driven valveless micropump, respectively. Muscle ring cultured by tissue engineering is assembled on a hydrogel tube fixed at both ends to PDMS scaffolds. The muscle ring is located off-center. Under electrical stimulation, the muscle ring contracts and squeezes the hydrogel tube, causing elastic waves to propagate along the tube and reflect back at the boundary between the soft/stiff tube boundaries. The asymmetric position of the muscle ring causes a time delay for the wave to reach the boundary and be reflected, causing a net unidirectional flow of liquid in the hydrogel tube, as schematically shown in Figure 8A (iii). The average flow velocity of the liquid in the tube exceeded 60 um/s under 4Hz electrical stimulation, as shown in Figure 8A (iv). The flow rate of this micropump can reach 22.5 uL/min, which is three orders of magnitude higher than the cardiomyocytes-driven micropump described previously. The proposal of this kind of micropump makes it

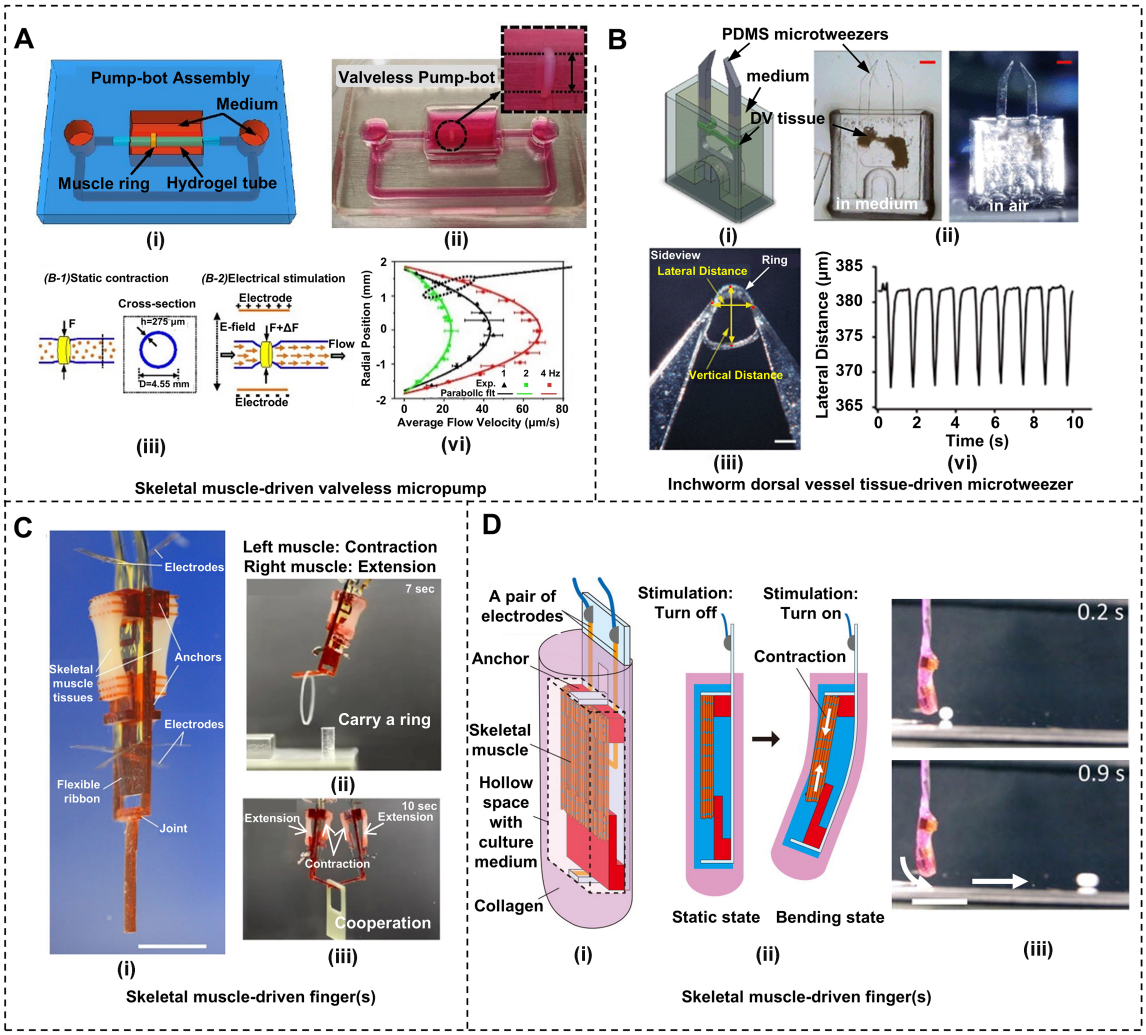

Figure 8. Strip-contraction-based non-locomotion bio-bots. (A) A skeletal muscle-driven valveless micropump. (i) Schematic of the assembled micropump by inserting the hydrogel tube into the round PDMS channels with a muscle ring wrapping around the tube at an off-center location; (ii) Photograph of the micropump; (iii) Schematic illustration of tube deformation under electrical stimulations; (iv) Flow patterns along the diameter of the tube at midsection under electrical stimulation of various frequencies. Reproduced with permission[88]. Copyright 2019, National Academy of Sciences; (B) A insect dorsal vessel tissue-driven microtweezer. (i) Schematic of the assembled microtweezer; (ii) Photographs of the microtweezer operated in medium (left) and in air (right) from the side; (iii) The microtweezer holding a tiny ring; (iv) Lateral displacement of the ring. Reproduced with permission[94]. Copyright 2013, RSC; (C) Skeletal muscle-driven fingers for pick-and-place manipulation of objects. (i) Photograph of the skeletal muscle-driven finger with the antagonistic pair of skeletal muscle tissues; (ii) The finger can carry a ring by selective contractions of the skeletal muscle tissues generated with electrical pulses; (iii) Two fingers can carry a square frame together. Reproduced with permission[96]. Copyright 2018, American Association for the Advancement of Science; (D) A skeletal muscle-driven finger encapsulated with collagen. (i) Schematic of the assembled skeletal muscle-driven finger; (ii) Operating principle of the skeletal muscle-driven finger; (iii) The finger can bounce the tiny ball. Reproduced with permission[97]. Copyright 2020, AIP Publishing.

possible to actively control muscles to drive fluid movement. The circulation of fluid will form a feedback loop. If neurological drugs such as acetylcholine are introduced, the micropump will be able to respond to signals in the flowing liquid and manage pumping performance adaptively based on the feedback[89,90].

Soft gripping bio-bots can manipulate objects smoothly and gently. Akiyama *et al.* proposed an inchworm dorsal vessel tissue-driven microtweezer[94], which is a capsule made of a small amount of culture medium wrapped in the insect dorsal vessel tissue, as shown in Figure 8B (i). The microtweezer can work in medium

and air, as shown in Figure 8B (ii). Figure 8B (iii) shows its use to hold a small fluorinated ethylene propylene ring. As the dorsal vessel tissues contract at a frequency of 1.1Hz, the lateral distance of the ring decreases and recovers at the same frequency, and the vertical distance increases and recovers at the same frequency as well, as shown in Figure 8B (iv). By encapsulating the capsules with paraffin wax, the lifespan of the microtweezer is extended to more than 5 days. The operation of insect muscle tissue in an air environment provides great potential for the proposal of more biohybrid actuators in the future.

In addition to the microtweezer, in 2010, Kabumoto *et al.* proposed a skeletal muscle-driven soft gripper with almost the same dynamics as a neuromuscular control system[95]. The system includes a complete electromyogram signal acquisition system and a micro-gripper assembled from living skeletal muscles and PDMS skeleton. By converting the electromyographic signal into an electrical stimulation signal for stimulating skeletal muscles, the gripper is successfully controlled. In order to more closely approximate real fingers, in 2018, Morimoto *et al.* developed a biohybrid finger actuated by an antagonistic pair of skeletal muscle tissues[96], as shown in Figure 8C (i). The finger skeleton consists of the finger body, anchors and joints. Skeletal muscle is anchored by the anchors and the joint of the finger is imitated. When selectively stimulated to contract, the skeletal muscle pulls the ribbon by pulling the anchors to rotate the finger through the joint. The design can prevent spontaneous contraction by balancing the tension of antagonistic tissues. As a demonstration, a single finger can pick and carry the ring, as shown in Figure 8C (ii), and two fingers work together to transport the square frame, as shown in Figure 8C (iii). To address the defect that skeletal muscle tissue cannot be exposed to the air for a long time, Morimoto *et al.* wrapped the biohybrid finger in collagen[97], as shown in Figure 8D (i), so that the skeletal muscle tissue and the finger can move in the air. Figure 8D (ii) shows the operating principle; the finger can switch between the static state and bending state with the electric stimulation on and off. As a demonstration, the finger was driven to bounce a ball in the air, as shown in Figure 8D (iii). These bio-hybrid fingers closely match those of a living body and usually do not require high-energy input.

CONCLUSION AND OUTLOOK

With the continuous advancement of robotics technology, bio-bots have emerged as a significant development trend for the future. This paper illustrates two design principles of bio-bots, film-bending-based and strip-contraction-based strategies, and their advantages/limitations [Table 1]. The film-bending-based strategy provides a simple structural design and driving mechanism; however, it faces challenges in generating large and complex deformations, which limits the multifunctionality of bio-bots. In contrast, the strip-contraction-based strategy excels in force output and generating complex deformations, but it usually requires a more sophisticated structural design. This review provides a comprehensive overview of recent advances in bio-bots from a functional perspective, including walking, swimming and non-locomotion bio-bots, by exploring their structure designs and operational principles. The related bio-bots and their performances are summarized in Table 2. The bio-bots discussed in this review can be considered as preliminary explorations of practical applications, such as cardiomyocytes and skeletal muscle-driven biohybrid micropumps[85-90], cardiomyocytes-based microfluidic chips[92], bio-generator chips[93], targeted drug delivery and chemical or biological hazard detection. Despite significant advances of bio-bots in the past two decades, several challenges still exist for future developments:

(1) Advanced structural design with multifunctionalities.

While bionics provides a valuable approach for designing and developing bio-bots, it often presents challenges in design complexity to achieve multifunctionalities. Currently, most bio-bots exhibit only a single functionality. Advanced structure designs to develop a range of bio-bots capable of combining more

Table 1. Advantages, limitations, potential applications and future directions of current bio-bot technologies

Fundamentals of design principle	Advantages	Limitations	Potential applications	Future directions	Ref.
Film-bending-based	- Simple structural design - Better bending response - Suitable for small-scale motion - Adaptive to diverse environments	- Small deformation scale - Poor deformation modes	- Microfluidic pumps - Biosensors and miniature mechanical systems - Small-scale motion bio-bots for delivering and monitoring	- Improved force output and durability of muscle/film sheet - Enhanced structural design with multifunctionality - Extended lifespan	[57,58,60-62,70-76,83-87,91-93]
Strip-contraction-based	- Capable of generating larger forces - Suitable for macro-scale motion - Multiple deformation modes	- Requires complex mechanical structures - Challenges in synchronization and stress distribution with muscle tissue	- Microfluidic pumps - Soft grippers and fingers - Large-scale motion bio-bots for delivering and monitoring	- Advancement of tissue engineering techniques for enhanced muscle output - Adaptive contraction systems for various tasks - Extended lifespan	[63-69,77-82,88,94-97]

functionalities, operating in both land and water environments, and possessing multi-dwelling capabilities are highly desired.

(2) High power output.

Engineered muscles cultivated through tissue engineering typically generate forces on the order of micronewtons, resulting in micron-scale deformations, which limit their efficacy in achieving desired motions in macro-scale structures. Future work could focus on enhancing muscle output through advanced tissue engineering, such as directing muscle fiber growth by shaped molds or external stimuli[53,98], incorporating growth factors into culture mediums[67], *etc*.

(3) Long lifespan.

Existing bio-bots have a short lifespan, typically lasting only a few days, due to several reasons, such as the dissimilar environment to in vivo conditions, the limited self-repair of muscle recovery, *etc*. A long lifespan is important to make the bio-bot more competitive than conventional robots by pushing it to practical applications. Thus, more studies should pay attention to extending the lifespan of bio-bots.

The future advancement of bio-bots depends on continuous innovation in biological techniques, smart materials, and structural designs. The interdisciplinary collaboration among fields such as mechanics, materials, chemistry and biology will lead to the development of bio-bots with superior performance, enabling their widespread application in organ-on-a-chip systems, minimally invasive surgery, environmental monitoring, and beyond laboratory settings.

Table 2. Bio-bots with different functions

Types	Year	Performance: speed/function/flow rate	Control methods	Amplitude, Frequency	Ref.
Film-bending-based walking bio-bots	2005	16.52 BL/min	Spontaneous contraction	1.8 Hz	[57]
	2007	2.7 BL/min	Electrical stimulation	10 V, 1 Hz	[58]
	2007	4 BL/min	Spontaneous contraction	1.12 Hz	[60]
	2020	3.2 BL/min	Spontaneous contraction	1.2 Hz	[62]
Strip-contraction-based walking bio-bots	2014	1.5 BL/min	Electrical stimulation	20 V, 4 Hz	[67]
	2016	1.3 BL/min	Optical stimulation	1.9 mW/mm^2, 2 Hz	[69]
	2018	2.307 BL/min	Electrical stimulation	Not mentioned, 4 Hz	[68]
	2022	0.722 BL/min	Optical stimulation	2 mW/mm^2, 2 Hz	[65]
	2023	3.56 BL/min	Optical stimulation	10 W, 4 Hz	[64]
	2024	0.159 BL/min	Electrical stimulation	2 V/cm, 2 Hz	[63]
	2024	0.9 BL/min	Electrical stimulation	1.2 V/mm, 50 Hz	[66]
Film-bending-based swimming bio-bots	2007	4.36 BL/min	Electrical stimulation	10 V, 1 Hz	[58]
	2011	0.23 BL/min	Spontaneous contraction/chemical stimulation	0.25 Hz	[71]
	2012	24-42 BL/min	Electrical stimulation	5-10 V, 0.5-2 Hz	[70]
	2013	1.89 BL/min	Spontaneous contraction	3 Hz	[83]
	2016	14.8 BL/min	Optical stimulation	Not mentioned, 1.5 Hz	[72]
	2018	Not mentioned	Spontaneous contraction/ Electrical stimulation	0.5-6 V, 0.5/1/2 Hz	[74]
	2019	0.0871 BL/min	Spontaneous contraction	0.36 Hz	[84]
	2019	2.82 BL/min	Spontaneous contraction	1 Hz	[76]
	2022	0.996 BL/min	Spontaneous contraction/ Electrical stimulation	3.2 V, 0.7 Hz	[75]
	2022	64.3 BL/min	Spontaneous contraction/Optical stimulation	3.5 Hz	[73]
Strip-contraction-based swimming bio-bots	2014	0.291, 4.98 BL/min	Spontaneous contraction	2.2/3 Hz	[78]
	2016	1.03 BL/min	Spontaneous contraction	0.86 Hz	[82]
	2019	0.0131 BL/min	Optical stimulation	3.9 mW/mm^2, 1 Hz	[77]
	2021	2.77 BL/min	Electrical stimulation	15 V, 5 Hz	[81]
	2022	0.362 BL/min	Electrical stimulation	16 V, 2 Hz	[79]
	2024	0.008 BL/min	Electrical stimulation	10 V, 2 Hz	[80]
Film-bending-based non-locomotion bio-bots	2006	Pumping: 2 nL/min	Spontaneous contraction	0.7 Hz	[85]
	2007	Pumping: 0.047 μL/min	Spontaneous contraction	0.6 Hz	[86]
	2007	Pumping: 0.226 nL/min	Spontaneous contraction	0.2-0.4 Hz	[87]
	2019	Actuating	Electrical stimulation	40 V, 1-3 Hz	[91]
	2016	Avg. voltage: 200 mV	Spontaneous contraction	1.1 Hz	[92]
	2018	Concentration detection	Spontaneous contraction	0.6 Hz	[93]
Strip-contraction-based non-locomotion bio-bots	2010	Gripping	Electrical stimulation	50 V, 1, 10 Hz	[95]
	2013	Gripping	Spontaneous contraction	0.8-1.1 Hz	[94]
	2018	Pumping: 22.5 μL/min	Electrical stimulation	9 V, 4 Hz	[88]
	2018	Finger	Electrical stimulation	1.5 V/mm, 1/50 Hz	[96]
	2020	Finger	Electrical stimulation	2.5-6 V/mm, 1/20/50 Hz	[97]

DECLARATIONS

Authors' contributions

Conceptualization and supervision: Song J
Prepared the figures and wrote the article: He S, Liu S, Li X, Ye M
Revised and corrected the article: Song J, Wu H

Availability of data and materials

Not applicable.

Financial support and sponsorship

This work was supported by the National Natural Science Foundation of China (Grant Nos. 12321002, 12225209 and 12372168) and the "Pioneer" and "Leading Goose" R&D Program of Zhejiang (Grant No. 2023C01051).

Conflicts of interest

All authors declared that there are no conflicts of interest.

Ethical approval and consent to participate

Not applicable.

Consent for publication

Not applicable.

REFERENCES

1. Chan, V.; Asada, H. H.; Bashir, R. Utilization and control of bioactuators across multiple length scales. *Lab. Chip.* **2014**, *14*, 653-70. DOI PubMed
2. Semini, C.; Tsagarakis, N. G.; Guglielmino, E.; Focchi, M.; Cannella, F.; Caldwell, D. G. Design of HyQ - a hydraulically and electrically actuated quadruped robot. *Proc. Inst. Mech. Eng. Part. I. J. Syst. Control. Eng.* **2011**, *225*, 831-49. DOI
3. Hutter, M.; Gehring, C.; Lauber, A.; et al. ANYmal - toward legged robots for harsh environments. *Adv. Robot.* **2017**, *31*, 918-31. DOI
4. Kimura, H.; Akiyama, S.; Sakurama, K. Realization of dynamic walking and running of the quadruped using neural oscillator. *Auton. Robot.* **1999**, *7*, 247-58. DOI
5. Biswal, P.; Mohanty, P. K. Development of quadruped walking robots: a review. *Ain. Shams. Eng. J.* **2021**, *12*, 2017-31. DOI
6. Fan, Y.; Pei, Z.; Wang, C.; Li, M.; Tang, Z.; Liu, Q. A review of quadruped robots: structure, control, and autonomous motion. *Adv. Intell. Syst.* **2024**, *6*, 2300783. DOI
7. Ha, S. Quadrupedal robots trot into the wild. *Sci. Robot.* **2020**, *5*, eabe5218. DOI PubMed
8. Kim, D. Quadruped robots venture into the wild with open eyes. *Sci. Robot.* **2022**, *7*, eabn6798. DOI PubMed
9. Marquet, F.; Krut, S.; Company, O.; Pierrot, F. ARCHI: a new redundant parallel mechanism - modeling, control and first results. In *Proceedings 2001 IEEE/RSJ International Conference on Intelligent Robots and Systems*, Maui, USA, October 29, 2001 - November 03, 2001; Publisher: IEEE; pp 183-188. DOI
10. Gravagne, I.A.; Walker, I.D. On the kinematics of remotely-actuated continuum robots. In *Proceedings of the 2000 IEEE International Conference on Robotics and Automation 2000 ICRA. Millennium Conference*, San Francisco, USA, April 24-28, 2000; Publisher: IEEE; pp 2544-50. DOI
11. Burgner-kahrs, J.; Rucker, D. C.; Choset, H. Continuum robots for medical applications: a survey. *IEEE. Trans. Robot.* **2015**, *31*, 1261-80. DOI
12. Pfeifer, R.; Lungarella, M.; Iida, F. Self-organization, embodiment, and biologically inspired robotics. *Science* **2007**, *318*, 1088-93. DOI PubMed
13. Guo, B.; Wang, P.; Zhao, Z.; Duan, S.; Lei, H. Design and experiments of an origami-inspired pneumatic flexible manipulator. *Acta. Mech. Solida. Sin.* **2023**, *36*, 254-61. DOI
14. Teoh, Z.E.; Fuller, S.B.; Chirarattananon, P.; Prez-Arancibia, N.O.; Greenberg, J.D.; Wood, R.J. A hovering flapping-wing microrobot

with altitude control and passive upright stability. In *2012 IEEE/RSJ International Conference on Intelligent Robots and Systems*, Vilamoura-Algarve, Portugal, October 7-12, 2012; Publisher: IEEE; pp 3209-16. DOI

15. Morrow, J.; Shin, H.S.; Phillips-Grafflin, C. Improving soft pneumatic actuator fingers through integration of soft sensors, position and force control, and rigid fingernails. In *2016 IEEE International Conference on Robotics and Automation*, Stockholm, Sweden, May 16-21, 2016; Publisher: IEEE; pp 5024-503. DOI
16. Stokes, A. A.; Shepherd, R. F.; Morin, S. A.; Ilievski, F.; Whitesides, G. M. A hybrid combining hard and soft robots. *Soft. Robotics.* **2014**, *1*, 70-4. DOI
17. Li, T.; Li, G.; Liang, Y.; et al. Fast-moving soft electronic fish. *Sci. Adv.* **2017**, *3*, e1602045. DOI PubMed PMC
18. Shintake, J.; Rosset, S.; Schubert, B.; Floreano, D.; Shea, H. Versatile soft grippers with intrinsic electroadhesion based on multifunctional polymer actuators. *Adv. Mater.* **2016**, *28*, 231-8. DOI PubMed
19. Shian, S.; Bertoldi, K.; Clarke, D. R. Dielectric elastomer based "grippers" for soft robotics. *Adv. Mater.* **2015**, *27*, 6814-9. DOI PubMed
20. Ji, X.; Liu, X.; Cacucciolo, V.; et al. An autonomous untethered fast soft robotic insect driven by low-voltage dielectric elastomer actuators. *Sci. Robot.* **2019**, *4*, eaaz6451. DOI PubMed
21. Yang, S.; Sharma, P. A tutorial on the stability and bifurcation analysis of the electromechanical behaviour of soft materials. *Appl. Mech. Rev.* **2023**, *75*, 044801. DOI
22. Xia, Y.; He, Y.; Zhang, F.; Liu, Y.; Leng, J. A review of shape memory polymers and composites: mechanisms, materials, and applications. *Adv. Mater.* **2021**, *33*, e2000713. DOI PubMed
23. Keneth E, Kamyshny A, Totaro M, Beccai L, Magdassi S. 3D printing materials for soft robotics. *Adv. Mater.* **2021**, *33*, e2003387. DOI PubMed
24. Zhang, C.; Chen, G.; Zhang, K.; Jin, B.; Zhao, Q.; Xie, T. Repeatedly programmable liquid crystal dielectric elastomer with multimodal actuation. *Adv. Mater.* **2024**, *36*, e2313078. DOI PubMed
25. Ni, C.; Chen, D.; Yin, Y.; et al. Shape memory polymer with programmable recovery onset. *Nature* **2023**, *622*, 748-53. DOI PubMed
26. Wang, C.; Sim, K.; Chen, J.; et al. Soft ultrathin electronics innervated adaptive fully soft robots. *Adv. Mater.* **2018**, *30*, 1870087. DOI
27. He, Q.; Wang, Z.; Song, Z.; Cai, S. Bioinspired design of vascular artificial muscle. *Adv. Mater. Technol.* **2019**, *4*, 1800244. DOI
28. He, Q.; Wang, Z.; Wang, Y.; Song, Z.; Cai, S. Recyclable and self-repairable fluid-driven liquid crystal elastomer actuator. *ACS. Appl. Mater. Interfaces.* **2020**, *12*, 35464-74. DOI PubMed
29. He, Q.; Wang, Z.; Wang, Y.; Minori, A.; Tolley, M. T.; Cai, S. Electrically controlled liquid crystal elastomer-based soft tubular actuator with multimodal actuation. *Sci. Adv.* **2019**, *5*, eaax5746. DOI PubMed PMC
30. Ramezani, A.; Chung, S. J.; Hutchinson, S. A biomimetic robotic platform to study flight specializations of bats. *Sci. Robot.* **2017**, *2*, eaal2505. DOI PubMed
31. Karásek, M.; Muijres, F. T.; De, W. C.; Remes, B. D. W.; de, C. G. C. H. E. A tailless aerial robotic flapper reveals that flies use torque coupling in rapid banked turns. *Science* **2018**, *361*, 1089-94. DOI PubMed
32. Li, G.; Chen, X.; Zhou, F.; et al. Self-powered soft robot in the Mariana Trench. *Nature* **2021**, *591*, 66-71. DOI
33. Yin, C.; Wei, F.; Fu, S.; et al. Visible light-driven jellyfish-like miniature swimming soft robot. *ACS. Appl. Mater. Interfaces.* **2021**, *13*, 47147-54. DOI PubMed
34. Ren, Z.; Hu, W.; Dong, X.; Sitti, M. Multi-functional soft-bodied jellyfish-like swimming. *Nat. Commun.* **2019**, *10*, 2703. DOI PubMed PMC
35. Wang, Y.; Wang, Q.; Liu, M.; et al. Insect-scale jumping robots enabled by a dynamic buckling cascade. *Proc. Natl. Acad. Sci. U. S. A.* **2023**, *120*, e2210651120. DOI PubMed PMC
36. Chen, R.; Yuan, Z.; Guo, J.; et al. Legless soft robots capable of rapid, continuous, and steered jumping. *Nat. Commun.* **2021**, *12*, 7028. DOI PubMed PMC
37. Di, Y.; Zhang, Y.; Wen, Y.; et al. Inchworm-inspired soft robot with controllable locomotion based on self-sensing of deformation. *IEEE. Robot. Autom. Lett.* **2024**, *9*, 4345-52. DOI
38. Zhang, Z.; Wang, X.; Wang, S.; Meng, D.; Liang, B. Design and modeling of a parallel-pipe-crawling pneumatic soft robot. *IEEE. Access.* **2019**, *7*, 134301-17. DOI
39. Sun, Y.; Li, D.; Wu, M.; et al. Origami-inspired folding assembly of dielectric elastomers for programmable soft robots. *Microsyst. Nanoeng.* **2022**, *8*, 37. DOI PubMed PMC
40. Sitti, M. Miniature soft robots - road to the clinic. *Nat. Rev. Mater.* **2018**, *3*, 74-5. DOI
41. Cianchetti, M.; Laschi, C.; Menciassi, A.; Dario, P. Biomedical applications of soft robotics. *Nat. Rev. Mater.* **2018**, *3*, 143-53. DOI
42. Pena-Francesch, A.; Jung, H.; Demirel, M. C.; Sitti, M. Biosynthetic self-healing materials for soft machines. *Nat. Mater.* **2020**, *19*, 1230-5. DOI PubMed PMC
43. Yang, G. Z.; Bellingham, J.; Dupont, P. E.; et al. The grand challenges of *Science Robotics*. *Sci. Robot.* **2018**, *3*, eaar7650. DOI PubMed
44. Raman, R.; Grant, L.; Seo, Y.; et al. Damage, healing, and remodeling in optogenetic skeletal muscle bioactuators. *Adv. Healthc. Mater.* **2017**, *6*, 1700030. DOI PubMed PMC
45. Wang, W.; Duan, W.; Ahmed, S.; Mallouk, T. E.; Sen, A. Small power: autonomous nano- and micromotors propelled by self-generated gradients. *Nano. Today.* **2013**, *8*, 531-54. DOI
46. Sakar, M. S.; Neal, D.; Boudou, T.; et al. Formation and optogenetic control of engineered 3D skeletal muscle bioactuators. *Lab. Chip.*

2012, *12*, 4976-85. DOI PubMed PMC
47. Legant, W. R.; Pathak, A.; Yang, M. T.; Deshpande, V. S.; McMeeking, R. M.; Chen, C. S. Microfabricated tissue gauges to measure and manipulate forces from 3D microtissues. *Proc. Natl. Acad. Sci. U. S. A.* **2009**, *106*, 10097-102. DOI PubMed PMC
48. Bajaj, P.; Reddy, B. J.; Millet, L.; et al. Patterning the differentiation of C2C12 skeletal myoblasts. *Integr. Biol.* **2011**, *3*, 897-909. DOI PubMed
49. Leng, Y.; Li, X.; Zheng, F.; et al. Advances in in vitro models of neuromuscular junction: focusing on organ-on-a-chip, organoids, and biohybrid robotics. *Adv. Mater.* **2023**, *35*, e2211059. DOI
50. Gao, C.; Shi, Q.; Pan, X.; et al. Neuromuscular organoids model spinal neuromuscular pathologies in C9orf72 amyotrophic lateral sclerosis. *Cell. Rep.* **2024**, *43*, 113892. DOI PubMed
51. Aydin, O.; Passaro, A. P.; Elhebeary, M.; et al. Development of 3D neuromuscular bioactuators. *APL. Bioeng.* **2020**, *4*, 016107. DOI PubMed PMC
52. Shin, M. K.; Bang, J. S.; Lee, J. E.; et al. Generation of skeletal muscle organoids from human pluripotent stem cells to model myogenesis and muscle regeneration. *Int. J. Mol. Sci.* **2022**, *23*, 5108. DOI PubMed PMC
53. Raman, R.; Cvetkovic, C.; Bashir, R. A modular approach to the design, fabrication, and characterization of muscle-powered biological machines. *Nat. Protoc.* **2017**, *12*, 519-33. DOI PubMed
54. Gapinske, L.; Clark, L.; Caro-Rivera, L. M.; Bashir, R. Cryopreservation alters tissue structure and improves differentiation of engineered skeletal muscle. *Tissue. Eng. Part. A.* **2023**, *29*, 557-68. DOI PubMed
55. Mestre, R.; Fuentes, J.; Lefaix, L.; et al. Improved performance of biohybrid muscle□based bio□bots doped with piezoelectric boron nitride nanotubes. *Adv. Materials. Technologies.* **2023**, *8*, 2200505. DOI
56. Kaufman, C. D.; Liu, S. C.; Cvetkovic, C.; et al. Emergence of functional neuromuscular junctions in an engineered, multicellular spinal cord-muscle bioactuator. *APL. Bioeng.* **2020**, *4*, 026104. DOI PubMed PMC
57. Xi, J.; Schmidt, J. J.; Montemagno, C. D. Self-assembled microdevices driven by muscle. *Nat. Mater.* **2005**, *4*, 180-184. DOI PubMed
58. Feinberg, A. W.; Feigel, A.; Shevkoplyas, S. S.; Sheehy, S.; Whitesides, G. M.; Parker, K. K. Muscular thin films for building actuators and powering devices. *Science* **2007**, *317*, 1366-70. DOI PubMed
59. Chan, V.; Park, K.; Collens, M. B.; Kong, H.; Saif, T. A.; Bashir, R. Development of miniaturized walking biological machines. *Sci. Rep.* **2012**, *2*, 857. DOI PubMed PMC
60. Kim, J.; Park, J.; Yang, S.; et al. Establishment of a fabrication method for a long-term actuated hybrid cell robot. *Lab. Chip.* **2007**, *7*, 1504-8. DOI PubMed
61. Kim, T. H.; Kwon, C. H.; Lee, C.; et al. Bio-inspired hybrid carbon nanotube muscles. *Sci. Rep.* **2016**, *6*, 26687. DOI PubMed PMC
62. Sun, L.; Chen, Z.; Bian, F.; Zhao, Y. Bioinspired soft robotic caterpillar with cardiomyocyte drivers. *Adv. Funct. Mater.* **2020**, *30*, 1907820. DOI
63. Zhang, C.; Yang, L.; Wang, W.; et al. Steering muscle-based bio-syncretic robot through bionic optimized biped mechanical design. *Soft. Robot.* **2024**, *11*, 484-93. DOI PubMed
64. Kim, Y.; Yang, Y.; Zhang, X.; et al. Remote control of muscle-driven miniature robots with battery-free wireless optoelectronics. *Sci. Robot.* **2023**, *8*, eadd1053. DOI PubMed
65. Wang, J.; Wang, Y.; Kim, Y.; Yu, T.; Bashir, R. Multi-actuator light-controlled biological robots. *APL. Bioeng.* **2022**, *6*, 036103. DOI PubMed PMC
66. Kinjo, R.; Morimoto, Y.; Jo, B.; Takeuchi, S. Biohybrid bipedal robot powered by skeletal muscle tissue. *Matter* **2024**, *7*, 948-62. DOI
67. Cvetkovic, C.; Raman, R.; Chan, V.; et al. Three-dimensionally printed biological machines powered by skeletal muscle. *Proc. Natl. Acad. Sci. U. S. A.* **2014**, *111*, 10125-30. DOI PubMed PMC
68. Pagan-diaz, G. J.; Zhang, X.; Grant, L.; et al. Simulation and fabrication of stronger, larger, and faster walking biohybrid machines. *Adv. Funct. Mater.* **2018**, *28*, 1801145. DOI
69. Raman, R.; Cvetkovic, C.; Uzel, S. G.; et al. Optogenetic skeletal muscle-powered adaptive biological machines. *Proc. Natl. Acad. Sci. U. S. A.* **2016**, *113*, 3497-502. DOI PubMed PMC
70. Nawroth, J. C.; Lee, H.; Feinberg, A. W.; et al. A tissue-engineered jellyfish with biomimetic propulsion. *Nat. Biotechnol.* **2012**, *30*, 792-7. DOI PubMed PMC
71. Takemura, R.; Akiyama, Y.; Hoshino, T.; Morishima, K. Chemical switching of jellyfish-shaped micro robot consisting only of cardiomyocyte gel. In *16th International Solid-State Sensors, Actuators and Microsystems Conference*, Beijing, China, June 5-9, 2011; Publisher: IEEE; pp 2442-5. DOI
72. Park, S. J.; Gazzola, M.; Park, K. S.; et al. Phototactic guidance of a tissue-engineered soft-robotic ray. *Science* **2016**, *353*, 158-62. DOI PubMed PMC
73. Lee, K. Y.; Park, S. J.; Matthews, D. G.; et al. An autonomously swimming biohybrid fish designed with human cardiac biophysics. *Science* **2022**, *375*, 639-47. DOI PubMed PMC
74. Shin, S. R.; Migliori, B.; Miccoli, B.; et al. Electrically driven microengineered bioinspired soft robots. *Adv. Mater.* **2018**, *30*, 1704189. DOI PubMed PMC
75. Tetsuka, H.; Pirrami, L.; Wang, T.; Demarchi, D.; Shin, S. R. Wirelessly powered 3D printed hierarchical biohybrid robots with multiscale mechanical properties. *Adv. Funct. Mater.* **2022**, *32*, 2202674. DOI PubMed PMC
76. Xu, B.; Han, X.; Hu, Y.; et al. A remotely controlled transformable soft robot based on engineered cardiac tissue construct. *Small*

2019, *15*, e1900006. DOI PubMed

77. Aydin, O.; Zhang, X.; Nuethong, S.; et al. Neuromuscular actuation of biohybrid motile bots. *Proc. Natl. Acad. Sci. U. S. A.* **2019**, *116*, 19841-7. DOI PubMed PMC
78. Williams, B. J.; Anand, S. V.; Rajagopalan, J.; Saif, M. T. A self-propelled biohybrid swimmer at low Reynolds number. *Nat. Commun.* **2014**, *5*, 3081. DOI
79. Zhang, C.; Zhang, Y.; Wang, W.; Xi, N.; Liu, L. A manta ray-inspired biosyncretic robot with stable controllability by dynamic electric stimulation. *Cyborg. Bionic. Syst.* **2022**, *2022*, 2022/9891380. DOI
80. He, S.; Zhou, Y.; Wu, Y.; Li, Z.; Song, J. A spring-shaped biohybrid swimmer powered by engineered skeletal muscle. *Sci. Sin-Phys. Mech. As.* **2024**, *54*, 264509. (in Chinese). DOI
81. Guix, M.; Mestre, R.; Patiño, T.; et al. Biohybrid soft robots with self-stimulating skeletons. *Sci. Robot.* **2021**, *6*, eabe7577. DOI PubMed
82. Holley, M. T.; Nagarajan, N.; Danielson, C.; Zorlutuna, P.; Park, K. Development and characterization of muscle-based actuators for self-stabilizing swimming biorobots. *Lab. Chip.* **2016**, *16*, 3473-84. DOI PubMed
83. Shin, S. R.; Jung, S. M.; Zalabany, M.; et al. Carbon-nanotube-embedded hydrogel sheets for engineering cardiac constructs and bioactuators. *ACS. Nano.* **2013**, *7*, 2369-80. DOI PubMed PMC
84. Yalikun, Y.; Uesugi, K.; Hiroki, M.; et al. Insect muscular tissue-powered swimming robot. *Actuators* **2019**, *8*, 30. DOI
85. Tanaka, Y.; Morishima, K.; Shimizu, T.; et al. An actuated pump on-chip powered by cultured cardiomyocytes. *Lab. Chip.* **2006**, *6*, 362-8. DOI
86. Tanaka, Y.; Sato, K.; Shimizu, T.; Yamato, M.; Okano, T.; Kitamori, T. A micro-spherical heart pump powered by cultured cardiomyocytes. *Lab. Chip.* **2007**, *7*, 207-12. DOI PubMed
87. Park, J.; Kim, I. C.; Baek, J.; et al. Micro pumping with cardiomyocyte-polymer hybrid. *Lab. Chip.* **2007**, *7*, 1367-70. DOI PubMed
88. Li, Z.; Seo, Y.; Aydin, O.; et al. Biohybrid valveless pump-bot powered by engineered skeletal muscle. *Proc. Natl. Acad. Sci. U. S. A.* **2019**, *116*, 1543-8. DOI PubMed PMC
89. Li, Z.; Balance, W. C.; Joy, M. S. H.; et al. Adaptive biohybrid pumping machine with flow loop feedback. *Biofabrication* **2022**, *14*, 025009. DOI PubMed
90. Li, Z.; Saif, M. T. A. Mechanics of biohybrid valveless pump-bot. *Journal. of. Applied. Mechanics.* **2021**, *88*, 111004. DOI
91. Hasebe, A.; Suematsu, Y.; Takeoka, S.; et al. Biohybrid actuators based on skeletal muscle-powered microgrooved ultrathin films consisting of poly(styrene-*block*-butadiene-*block*-styrene). *ACS. Biomater. Sci. Eng.* **2019**, *5*, 5734-43. DOI PubMed
92. Liu, X.; Zhao, H.; Lu, Y.; et al. *In vitro* cardiomyocyte-driven biogenerator based on aligned piezoelectric nanofibers. *Nanoscale* **2016**, *8*, 7278-86. DOI PubMed
93. Fu, F.; Shang, L.; Chen, Z.; Yu, Y.; Zhao, Y. Bioinspired living structural color hydrogels. *Sci. Robot.* **2018**, *3*, eaar8580. DOI PubMed
94. Akiyama, Y.; Sakuma, T.; Funakoshi, K.; Hoshino, T.; Iwabuchi, K.; Morishima, K. Atmospheric-operable bioactuator powered by insect muscle packaged with medium. *Lab. Chip.* **2013**, *13*, 4870-80. DOI PubMed
95. Kabumoto, K.; Hoshino, T.; Morishima, K. Bio-robotics using interaction between neuron and muscle for development of living prosthesis. In *Proceedings of the 2010 3rd IEEE RAS and EMBS International Conference on Biomedical Robotics and Biomechatronics*, Tokyo, Japan, September 26-29, 2010; Publisher: IEEE; pp 419-24. DOI
96. Morimoto, Y.; Onoe, H.; Takeuchi, S. Biohybrid robot powered by an antagonistic pair of skeletal muscle tissues. *Sci. Robot.* **2018**, *3*, eaat4440. DOI PubMed
97. Morimoto, Y.; Onoe, H.; Takeuchi, S. Biohybrid robot with skeletal muscle tissue covered with a collagen structure for moving in air. *APL. Bioeng.* **2020**, *4*, 026101. DOI PubMed PMC
98. Liu, L.; Zhang, C.; Wang, W.; Xi, N.; Wang, Y. Regulation of C2C12 differentiation and control of the beating dynamics of contractile cells for a muscle-driven biosyncretic crawler by electrical stimulation. *Soft. Robot.* **2018**, *5*, 748-60. DOI PubMed